Structure, mechanical properties, and corrosion resistance of low-nickel nitrogen-alloyed austenite stainless steel

Sarkis Muradian [1,*], Yan Sun [1], Qian Zhong [1], Mingzhou Liu [1], Chen Su [1], Wenqiang Sun [1]

[1] R&D center, Zhejiang JIULI Hi-tech metals Co, Ltd, Huzhou, China; info@jiuli.com

* Correspondence: sarkis@jiuli.com

(Received 09 October 2025; Accepted 07 May 2026)

Abstract

This study investigates the structure, mechanical properties, and corrosion resistance of low-nickel nitrogen-alloyed austenitic stainless steels (Cr17Mn9Ni3N, 05Cr18Mn10Ni3N) as cost-effective alternatives to conventional AISI 304L and AISI 321 grades. The alloys were smelted in vacuum induction melting with nitrogen introduced via nitrided ferrochrome. Microstructural analysis confirmed fully austenitic structures with finer grain sizes (ASTM No. 4.5–6.0) compared to conventional steels (ASTM No. 3.5–4.0). Mechanical testing revealed superior yield strength (~414 MPa) and tensile strength (~730–748 MPa) in nitrogen-alloyed steels, attributed to solid-solution strengthening by nitrogen. However, the impact toughness at cryogenic temperatures (-196°C) was reduced, and brittle facets were found on the fracture surface. The results of potentiodynamic polarization tests showed that AISI 304L steel exhibited a higher pitting potential. The pitting potentials of steels Cr17Mn9Ni3N and 05Cr18Mn10Ni3N were lower than that of AISI 304L but higher than that of AISI 321 steel. Economic analysis highlighted significant cost savings potential through nickel substitution with nitrogen. The results validate nitrogen-alloyed steels as viable alternatives for applications

requiring high strength and corrosion resistance, though cryogenic applications require careful nickel content optimization.

Keywords: low-nickel nitrogen-alloyed stainless steel; austenite stability; mechanical properties; corrosion, low-temperature toughness, cost-effectiveness

1. Introduction

Stainless steels are widely used across various industries due to their excellent corrosion resistance and mechanical properties. Among them, AISI 304 and its modifications (including AISI 321) dominate the market, accounting for approximately 60% of global stainless steel production. These austenitic grades, balanced with chromium and nickel, offer reliable performance in many environments [1-2]. However, the high and volatile cost of nickel has driven the search for cost-effective alternatives with comparable properties.

A common approach to addressing this issue is the use of AISI 201 steel. In this steel, the austenite-forming nickel is replaced by manganese, nitrogen, and carbon, while the content of ferrite-forming chromium is reduced from 18-20% to 16-18%, which is also done to preserve the austenitic structure. Accordingly, the decrease in chromium concentration and the increase in manganese and carbon concentrations, despite the higher nitrogen content, generally lead to reduced corrosion resistance. However, an principal advantage of this steel is its 20-30% lower production cost compared to AISI 304 steel and improved mechanical properties due to the increased nitrogen concentration [3-5].

In general, the addition of nitrogen in 200-series stainless steels not only compensates for the reduced nickel content but also significantly enhances their mechanical strength and structural performance [6-10]. Nitrogen acts as a potent

solid-solution strengthener, allowing these steels to achieve higher yield and tensile strength compared to conventional AISI 304. This makes them particularly suitable for high-stress applications, where increased load-bearing capacity enables the use of thinner cross-sections in components such as tubes, structural elements, and pressure vessels [11-14]. The reduction in material thickness, combined with nitrogen's positive effect on fatigue resistance and wear durability, improves the long-term reliability of constructions while simultaneously reducing overall weight. Since nitrogen-alloyed steels are also more cost-effective due to lower nickel content, their adoption leads to substantial cost savings – both in material expenses and through weight-optimized designs. Thus, the combination of superior mechanical properties, reduced weight, and lower production costs makes nitrogen-strengthened stainless steels an economically advantageous alternative to conventional austenitic grades [15-17].

Since the corrosion resistance of AISI 201 steel is insufficient compared to AISI 304-type steels, this work explores low-carbon alternatives to this steel. This article examines the structure, mechanical properties, and corrosion resistance of cost-effective nitrogen-alloyed austenitic steels in the Fe-Cr-Mn-Ni-N system with different carbon content ranging from 0.01 to 0.05 wt. %. During development, special attention was paid to balancing raw material costs against performance to maintain commercial viability while preserving a fully austenitic structure. The article compares these properties with those of conventional carbon-free stainless austenitic steels, such as AISI 304L and AISI 321. This study aims to validate the substitution of conventional steels with economically viable alternatives without compromising main performance characteristics.

While AISI 201-type steels offer a cost reduction through partial nickel substitution, they often suffer from reduced corrosion resistance and austenite

stability due to higher carbon and manganese contents. In contrast, the low-carbon, nitrogen-alloyed Cr17Mn9Ni3N and 05Cr18Mn10Ni3N grades investigated in this work achieve a more favorable balance between mechanical performance and corrosion resistance by optimizing the C–Cr–Mn–Ni–N system. These materials are specifically targeted at ambient-temperature structural applications – such as industrial tubing, high-pressure tubes and load-bearing components – where high strength and cost-effectiveness are required.

2. Materials and methods

2.1 Materials

The nitrogen-alloyed steels were smelted in a 25 kg vacuum induction furnace (VIM) using pure raw materials. After melting in vacuum, the nitriding process was carried out by adding nitrided ferrochrome into the molten steel under an argon atmosphere. Conventional steels ingots - AISI 321 and AISI 304L were provided to us from our suppliers. The chemical composition of the resulting ingots is shown in Table 1.

Table 1. Chemical composition of researched steels (wt. %)

N	Grade	C	Mn	Si	Ni	Cr	N	Cu	Ti	Al	O	Fe
1	Cr17Mn9Ni3N	0.01	8.93	0.43	3.54	16.88	0.29	0.0	0.004	0.0055	0.0039	bal
2	05Cr18Mn10Ni3N	0.05	10.33	0.38	3.28	17.6	0.31	0.0	0.006	0.0062	0.0055	
3	AISI 321	0.03	1.22	0.45	9.12	17.47	0.01	0.1	0.251	0.0324	0.0017	
4	AISI 304L	0.02	0.63	0.36	8.28	18.16	0.09	0.3	0.002	0.0029	0.0025	

Hot forging of all ingots was performed using a 5-ton press. The ingots were forged from a diameter of 100 mm down to 40 mm in 3–4 passes in temperature range from 1200 to 850°C. Subsequently, the obtained workpieces underwent heat treatment in a furnace at 1100 ˚C for 1 hour, followed by water cooling.

The chemical composition of the steel was analyzed according to the following standards: GB/T 11170-2008, GB/T 11261-2006, GB/T 20123-2006, GB/T 20124-2006, GB/T 223.82-2018, GB/T 23942-2009. The equipment used for the analysis: Carbon sulfur Analyzer HX-104-22, inductively coupled plasma emission spectrometer HX-103-38, hydrogen analyzer HX-204-61, oxygen and nitrogen analyzer HX-204-62, direct reading spectrometer HX-103-40.

2.2 Structural research

Calculations of the phase composition of steels were performed using the ThermoCalc software, database version TCFE11.

Metallographic examination was conducted according to the standards GB/T 6394-2017 "Determination of estimating the average grain size of metal", GB/T 10561-2005 "Steel-Determination of content of nonmetallic inclusions – Micrographic method using standards diagrams", GB/T 13298-2015 "Inspection methods of microstructure for metals", GB/T 13305-2008 "Micrographic method for determining area content of the α-phases in Stainless steels". Grain size measurements were performed using the linear intercept method in accordance with GB/T 6394-2017. In line with the standard practice for austenitic steels, twin boundaries were excluded from the intercept count. The equipment used for the analysis: optical microscope JX-102-30. Sampling in all cases was in the transverse direction. The etching process for the surface of the metal grinds was done with hydrochloric acid with hydrogen peroxide.

Thermofisher scanning electron microscope (SEM) Quattro S with an EDAX Elect Super EDX detector was used for the SEM and EDX analysis. The EDX analysis was carried out using the standard GB/T 18907-2013 "Microbeam analysis. Analytical electron microscopy. Selected-area electron diffraction analysis using a transmission electron microscope". Cross-section bulk samples were polished and etched to show the microstructures.

2.3 Mechanical properties

Room temperature tensile test was conducted in accordance with the standard GB/T 228.1-2021 “Metallic materials - Tensile testing- Part 1：Method of test at room temperature”, equipment type: tensile testing machine LX-102-49, sampling orientation - longitudinal, sample type - round bar, gage length - 25 mm. Toughness determination was conducted in accordance with the standard ASTM A370-2023 “Standard Test Methods and Definitions for Mechanical Testing of Steel Products” at room temperature, -50 and -196°C. Sampling direction - longitudinal, sample type – standard sample (width – 10 mm), Charpy Impact Test Specimens.

2.4 Corrosion tests

The corrosion performance of the steel samples was characterized through a suite of standardized test methods. For each steel grade, three specimens were tested to ensure reproducibility of the corrosion results. Pitting corrosion resistance was evaluated per ASTM G48-11, Method A, wherein ground specimens (25×50×4 mm, 80-grit finish) were immersed in 10% $FeCl_3 \cdot 6H_2O$ solution at 25°C for 10 hours. The extent of corrosion was quantified by mass loss measurement.

Intergranular corrosion was determined in accordance with ASTM A262-15, Practice B. Samples (20×25×4.5 mm) were prepared with an 80-grit surface finish and exposed to a 50% H_2SO_4 - $FeSO_4$ solution at 25°C for 10 hours, with degradation assessed via mass loss.

General corrosion resistance was tested following the JB/T 7901-1999 standard. Ground plates (25×50×4.75 mm, 80-grit) were subjected to a boiling 5% H_2SO_4 solution for 10 hours, and the corrosion rate was evaluated by mass loss.

Electrochemical characterization was carried out to determine the pitting potential (E_pit), as specified in GB/T 17899. These measurements were performed

in a 3.5% NaCl solution at 25°C at a scan rate of 0.5 mV/s, using a saturated calomel electrode (SCE) as the reference.

3. Results

The results of the study on austenitic nitrogen-alloyed steels were divided into three main sections: structure analysis, mechanical properties, and corrosion resistance. For comparison, commercially prevalent stainless steels AISI 321 and AISI 304L were also investigated.

3.1. Structure research

The study of the structure of steels began with the analysis of equilibrium phase diagrams using the Thermocalc software. The results of these calculations are shown in Figure 1.

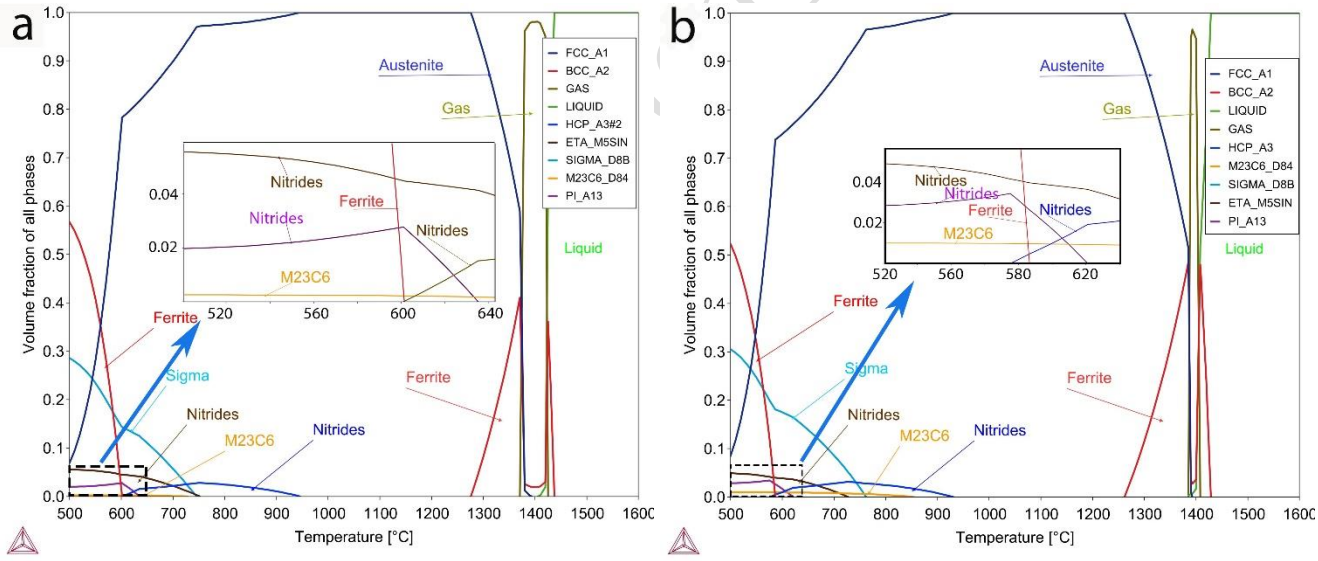

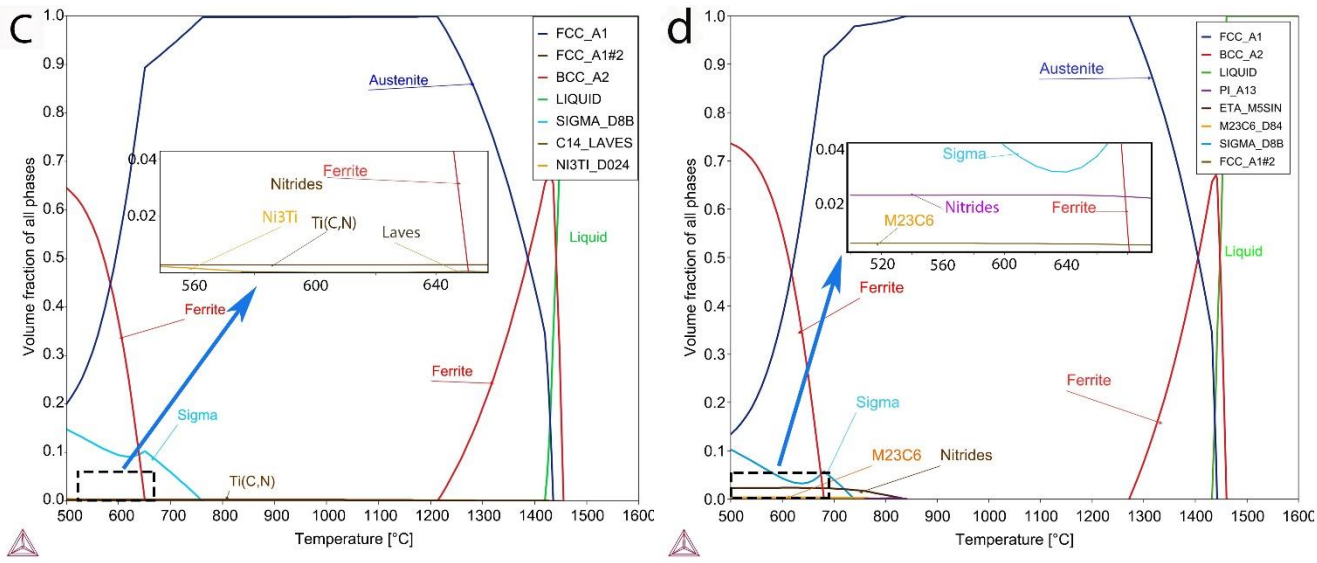

Figure 1. The equilibrium phase diagrams calculated by ThermoCalc for steels from Table 1: a – steel Cr17Mn9Ni3N, b – steel 05Cr18Mn10Ni3N, c - AISI 321, d - AISI 304L

According to diagrams all investigated steels solidify with formation of a significant ferrite fraction. In the nitrogen-alloyed steels, the ferrite fraction during solidification reaches: ~41% for steel Cr17Mn9Ni3N, ~50% for steel 05Cr18Mn10Ni3N. For AISI 321 steel, this fraction amounts to approximately 63%, while for AISI 304L steel it reaches 67%. This ratio indirectly indicates better stability of the austenite in nitrogen-alloyed steels.

However, the probability of sigma-phase formation in nitrogen-alloyed steels is higher than in conventional stainless steels. According to thermodynamic calculations, the sigma-phase formation temperature for nitrogen-alloyed steels ranges between 750-770°C, while for AISI 321 and AISI 304L steels it is approximately 730°C. At 500 ˚C, the sigma-phase fraction reaches up to 30 vol.% in nitrogen-alloyed steels, compared to only 10-13 vol.% in conventional steels.

Furthermore, due to the presence of nitrogen in nitrogen-alloyed steels, the equilibrium phase diagrams for these steels show a substantial fraction of nitride

phases in various forms. Depending on the nitrogen concentration, nitride precipitation begins at temperatures about 940°C and reaches a volume fraction of up to 5% at 500°C. Although the presence of 0.08 wt.% nitrogen in AISI 304L steel leads to the formation of a nitride phase on the phase diagram but in relatively small amounts

The equilibrium phase diagrams show that nitrogen-alloyed steels (Figure 1a,1b) under equilibrium conditions would crystallize with gas phase due to the formation of a substantial ferrite fraction during solidification. In practice, the steels did not exhibit porosity; however, the maximum permissible nitrogen concentration in solid metal relative to liquid metal was indeed reduced. In the liquid state, nitrogen concentrations up to 0.48% were achieved for these steels without visible boiling in the furnace. Nevertheless, during solidification with ferrite formation, nitrogen solubility in the metal drops sharply, leading to pore formation. Our experimental studies established that pore-free solidification of such steels occurs only at nitrogen concentrations below 0.35-0.3%, depending on the content of austenite-stabilizing elements (nickel, manganese, and carbon), which reduce the ferrite fraction during liquid metal crystallization.

Before the microstructure analysis, an examination of non-metallic inclusions was performed for all steels in the as-forged and final solid-solution heat-treated condition. The analysis results are presented in Table 2.

Table 2. Result of research for non-metallic inclusions by standard GB/T 10561-2005 A for steels from table 1.

N	Grade	Magnification	A		B		C		D	
			Thin	Heavy	Thin	Heavy	Thin	Heavy	Thin	Heavy
1	Cr17Mn9Ni3N	X100	0	0	0	0	0	0	2.0	0
2	05Cr18Mn10Ni3N		0	0	0	0	0	0	1.5	0
3	AISI321		0	0	0	0	0	0	2.0	0
4	AISI304L		0	0	0	0	0	0	1.0	0

The analysis shows minimal levels of globular oxide-type point inclusions in AISI 304L steel (1 point according to the GB/T 10561-2005 standard) and slightly higher values in the other steels (1.5, 2 points per GB/T 10561-2005). EDS analysis confirmed that the non-metallic inclusions in all steels consisted predominantly of aluminum oxides with the exception of AISI 321 steel, where a significant amount of titanium nitrides and carbides was also detected. The formation of these inclusions was attributed to the deoxidation of liquid steel with aluminum and titan stabilization (for steel AISI 321). Overall, the observed inclusion content is typical for steels produced via vacuum induction melting (VIM).

Figure 2 presents typical SEM images of the investigated steels' microstructure. The structure of all steels consisted of austenite, but despite identical forging regimes, the grain size (see Table 3) differed. For the nitrogen-alloyed steels (Figure 2 a,b), it ranged from 4.5 to 6.0 according to the GB/T 13305-2024 standard, while for the conventional AISI 321 and AISI 304L steels (Figure 2 d,e,f), it was 3.5 and 4.0, respectively. This microstructure is typical for austenitic steels after hot forging and subsequent solution annealing. The ferrite content was determined by

the optical method according to Standard GB/T 13305-2024, and the data are presented in Table 3. In all cases, no ferrite was detected by optical microscopy.

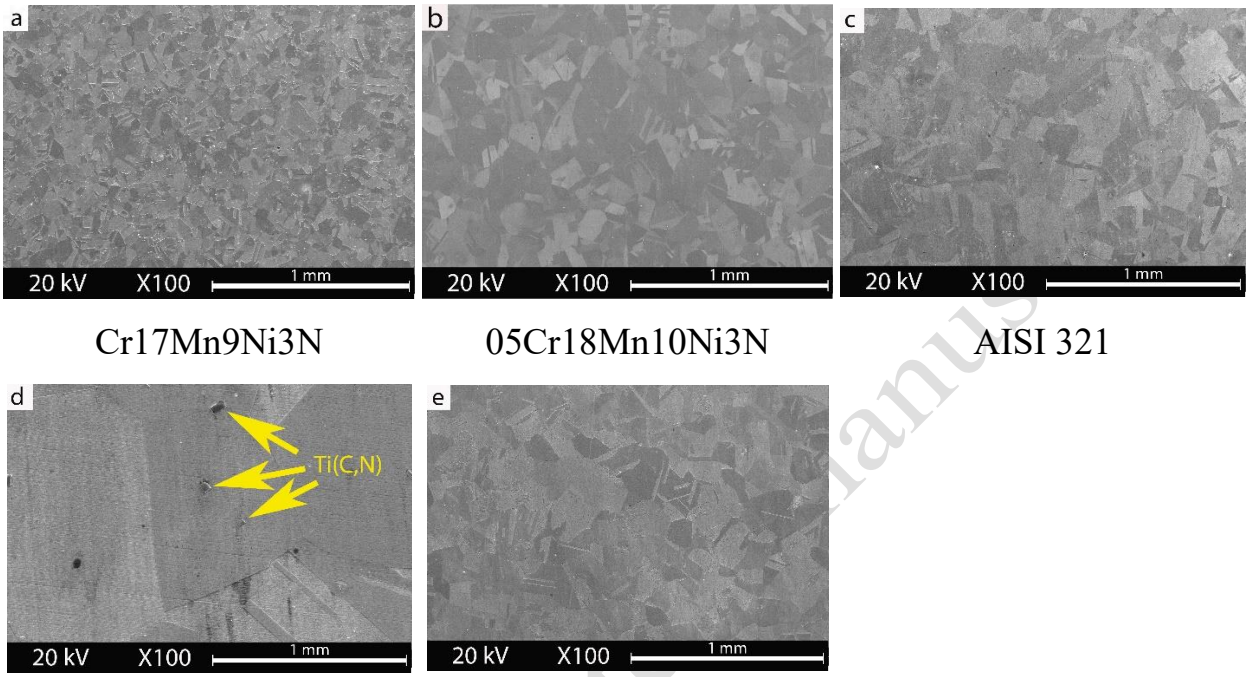

Cr17Mn9Ni3N | 05Cr18Mn10Ni3N | AISI 321

AISI 321 - Ti(C,N)-type particles | AISI 304L

Figure 2. SEM images of microstructure of researched steels: a – steel Cr17Mn9Ni3N X100, b – steel 05Cr18Mn10Ni3N X100, c - AISI 321 X100, d – AISI 321 X2500, e - AISI 304L X100 μm

Table 3. Grain size and ferrite content of researched steels

N	Grade	Grain size by standard ASTM E112-24	Ferrite content by standard GB/T 13305-2024, %
1	Cr17Mn9Ni3N	6.0	0
2	05Cr18Mn10Ni3N	4.5	
3	AISI321	3.5	
4	AISI304L	4.0	

Steel AISI 321 is stabilized with titanium. Its examination revealed numerous dispersed Ti(C,N)-type particles ranging in size from 1 to 10 μm (see Figure 2 d), which is a normal characteristic of this steel [1,2].

Except for differences in grain size and the presence of Ti(C,N)-type particles in AISI 321 steel, the microstructures of the steels differ only slightly. According to Thermo-Calc simulations, the nitrogen-alloyed steels in this work are better balanced in terms of the ratio of austenite- and ferrite-forming elements. The probability of high-temperature δ-ferrite formation in nitrogen-alloyed steels is lower than in conventional steels.

3.2. Mechanical properties

The results of tensile tests, Brinell hardness measurements, and Charpy impact toughness tests at room and low temperatures for the investigated steels are presented in Table 4. Engineering tensile stress–strain curves are shown in Figure 3.

Table 4. Mechanical properties of researched steels

N	Grade	Yield strength, MPa	Tensile strength, MPa	Elong., %	KCV, J			Hardness, HBW 2.5/187.5
					Room temp.	-50°C	-196°C	
	Cr17Mn9Ni3N	412	748	58	249	234	28	186
	05Cr18Mn10Ni3N	415	732	68	278	258	38	202
3	AISI321	206	553	67	330	332	183	119
4	AISI304L	258	592	75	360	336	193	142

As evident from the Figure 3, the nitrogen-alloyed steels exhibit significantly higher yield strength values (nearly twice as high as conventional steels) due to their elevated nitrogen content. Interestingly, in this case, the yield strength of AISI 304L steel is more than 50 MPa higher than that of AISI 321 steel, apparently also because of its increased nitrogen content and lower grain size.

AISI 304L steel demonstrates the highest ductility among the studied materials at 75%, while AISI 321 shows lower ductility at 67%. For the nitrogen-alloyed steels, elongation ranges between 58-68% and generally correlates with the grain size (see Table 3). Figure 3 also indicates that nitrogen-alloyed steels achieve better strength–ductility combination.

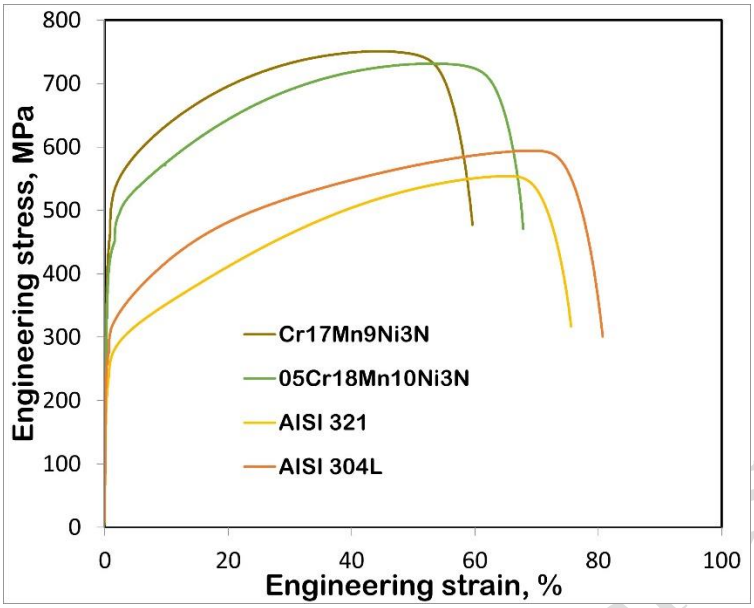

Figure 3. Engineering tensile stress–strain curves of researched steels.

The hardness of nitrogen-alloyed steels is significantly greater than that of conventional steels. As evident from Tables 1 and 4 in our study, hardness increases with higher concentrations of interstitial elements - carbon and nitrogen. After heat treatment at 1100 °C for 1 hour followed by water quenching, in accordance with the diagrams in Figure 1, both nitrogen and carbon distort the austenite crystal lattice, increasing its parameter and thereby enhancing the overall strength and hardness of austenite [18,19]. The 05Cr18Mn10Ni3N steel with the highest %C+%N content demonstrates the maximum hardness and AISI 321 steel with lowest %C+%N content – minimum. Additionally, the grain size of the investigated steels contributes to their hardness characteristics.

After tensile testing, the gauge sections of the AISI 304L and AISI 321 steel specimens became magnetic due to the formation of deformation-induced martensite, which is a well-known and thoroughly studied phenomenon for these steels [20]. In contrast, the gauge sections of the nitrogen-alloyed steels remained non-magnetic in all cases. The high austenite stability during deformation in these

steels is attributed to their elevated nitrogen and manganese contents [21,22]. This stability is determined by the M_{d30} temperature, the calculated values of which for the studied steels are presented in Table 5 according to formulas from [23].

Table 5. M_{d30} temperature calculated for researched steels

Sample number	Grade	M_{d30}
	Cr17Mn9Ni3N	-73
	05Cr18Mn10Ni3N	-114
3	AISI321	57
4	AISI304L	28

The M_{d30} temperature corresponds to the temperature at which 50% α′-martensite forms after 30% tensile deformation. The values in Table 5 indicate that the M_{d30} temperatures for nitrogen-alloyed steels are lower than -73°C and for AISI 321 and AISI 304L steels are 57°C and 28°C, respectively. Consequently, deformation of these steels at room temperature results in the formation of strain-induced martensite.

Figure 4 presents the impact toughness – temperature relationship for the investigated steels. The results reveal significant difference, particularly at -196°C. Nickel alloying is known to improve impact toughness, including at cryogenic temperatures, while nitrogen lowers the ductile-to-brittle transition temperature (DBTT) [18,24,25]. Grain size also substantially affects impact toughness [26].

Conventional steels contain higher nickel concentrations and lower nitrogen levels, with higher grain size numbers compared to nitrogen-alloyed steels. Consequently, those steels demonstrate much better impact toughness characteristics with a gradual, nearly imperceptible ductile-brittle transition. The performance

difference between AISI 321 and AISI 304L steels results from the elevated titanium (~0.25%) content in AISI 321 and the presence of hard titanium carbides/nitrides in its microstructure.

From Figure 4, it is evident that due to the reduced nickel content and elevated nitrogen concentration, the ductile-to-brittle transition in nitrogen-alloyed steels initiates above -196°C. Consequently, at this temperature, the specimens undergo brittle fracture, resulting in minimal impact toughness values. The difference between Cr17Mn9Ni3N and 05Cr18Mn10Ni3N steels is primarily determined by grain size. Similar effects for austenite stainless steels alloyed with nitrogen were reported in [19].

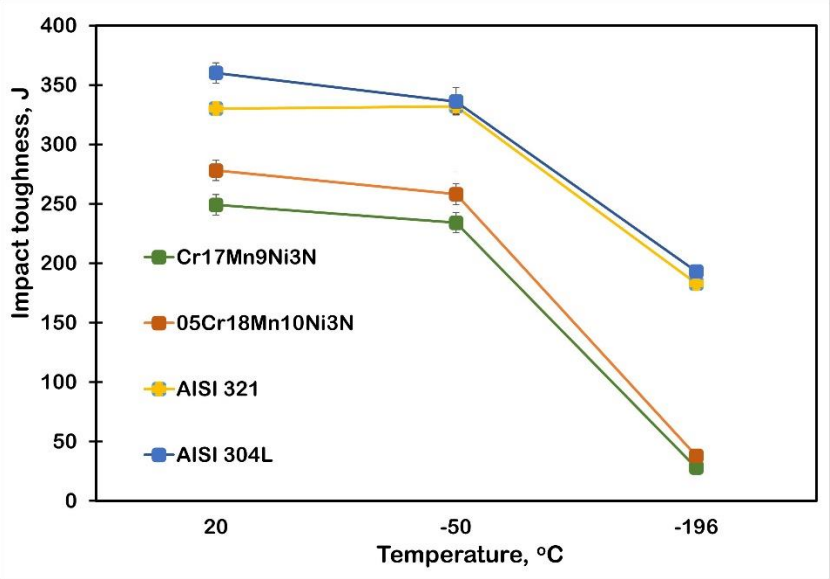

Figure 4. Impact toughness of researched steels in room and low temperatures

Fracture analyzes

The fracture of all investigated steels after impact testing at room temperature and -50°C had ductile dimpled fracture. However, significant differences were observed at -196°C (see Figure 5). In the conventional AISI 304L and AISI 321

steels, the fracture morphology also remained ductile. The difference between these steels lies only in the substantial number of Ti(C,N)-type particles at the crack propagation paths, which evidently reduce the total energy required for crack propagation (see Figure 5 d,e). Brittle facets were observed on the fracture surfaces of the nitrogen-alloyed steel samples (arrows in Figure 5 a,b). The size of such facets correlates with the grain size. These facets are formed by a slipping-off mechanism along active slip planes, not by cleavage associated with twinning [27].

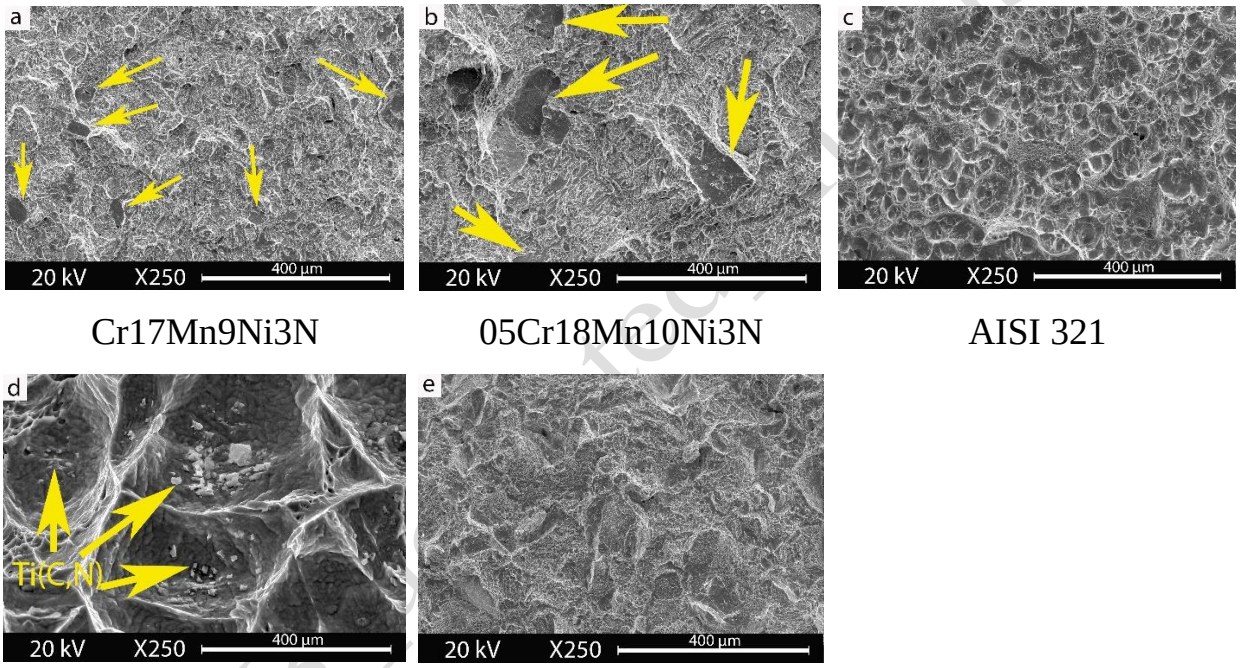

Cr17Mn9Ni3N 05Cr18Mn10Ni3N AISI 321

AISI 321 X2500 AISI 304L

Figure 5. Analysis of the fracture surfaces of Charpy impact test specimens tested at -196°C: a – steel Cr17Mn9Ni3N X250, b – steel 05Cr18Mn10Ni3N X250, c - AISI 321 X250, d – AISI 321 X2500, e - AISI 304L X250. Figures a and b, the arrows indicate brittle facets, figure d shows Ti(C,N) particles

3.3. Corrosion resistance

The electrochemical measurements depicted in Figure 6 and summarized in Table 6 reveal notable differences among the steels.

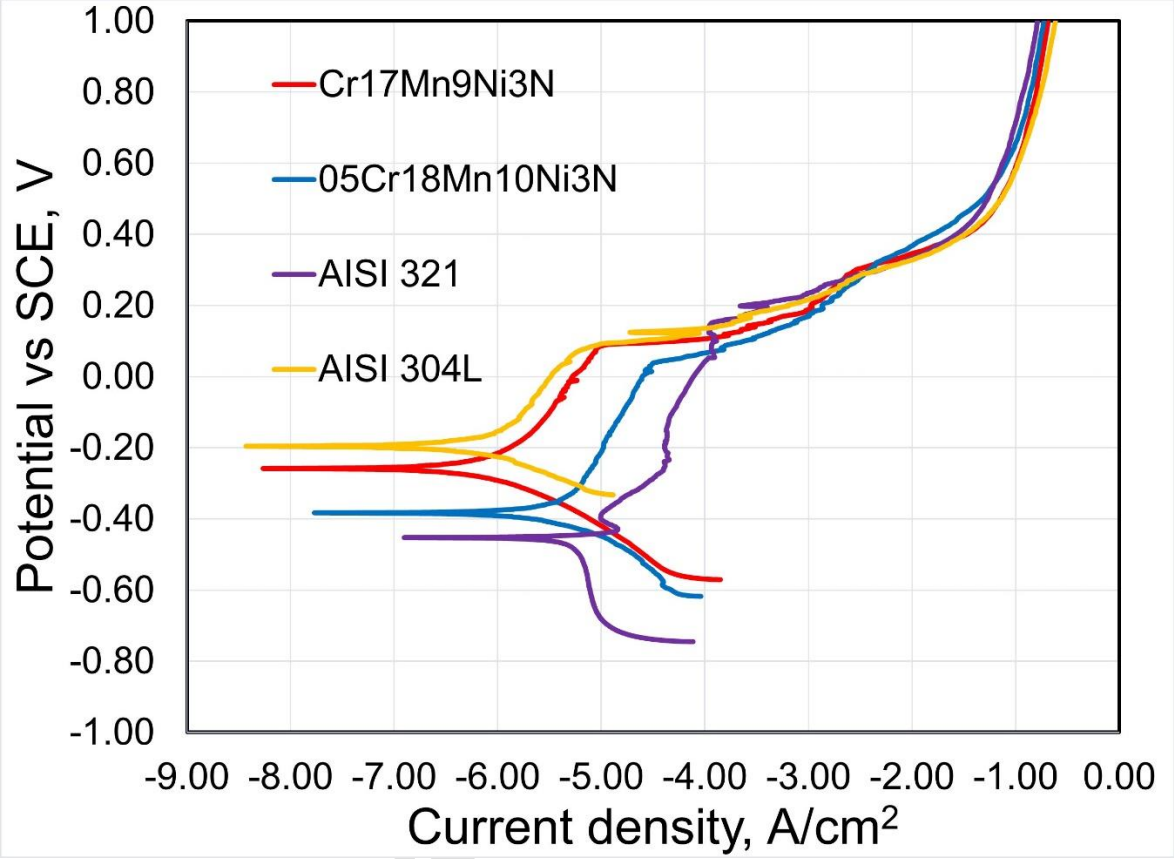

Figure 6. Polarization curves obtained in 3.5 wt.% NaCl solution for investigated steels.

AISI 304L steel exhibited a higher pitting potential than Cr17Mn9Ni3N and 05Cr18Mn10Ni3N steels, while AISI 321 steel demonstrated the lowest potential (this behavior for AISI 321 has been described in [28]). The difference in the corrosion behavior of Cr17Mn9Ni3N and 05Cr18Mn10Ni3N steels is evidently due to the influence of the increased carbon concentration and larger grain size in 05Cr18Mn10Ni3N steel. Overall, AISI 304L steel in comparison with nitrogen-alloyed steels in this test demonstrates good corrosion resistance performance.

Table 6. The results of electrochemical experiments.

Grade	E_{pit}, V
Cr17Mn9Ni3N	0.11
05Cr18Mn10Ni3N	0.07
AISI 321	0.05
AISI304L	0.14

4. Discussion

All investigated steels exhibited a fully austenitic microstructure after hot forging and solution annealing treatment. However, from the perspective of minimizing the risk of high-temperature δ-ferrite formation, the balance between austenite-stabilizing and ferrite-stabilizing elements is more optimally tuned in high-nitrogen steels. Thermo-Calc simulations confirmed that conventional steels exhibit a higher propensity for δ-ferrite formation, particularly during the initial solidification stage of ingot casting.

From the point of view of mechanical properties experimental results demonstrate that nitrogen-alloyed steels exhibit both advantages and disadvantages compared to conventional AISI 321 and AISI 304L steels. While nitrogen-alloyed steels possess superior strength and generally better strength-to-ductility ratios, their impact toughness at cryogenic temperatures reveals significant limitations. The superior strength parameters of nitrogen-alloyed steels directly correlate with increased hardness. This hardness enhancement significantly improves wear resistance, as demonstrated in numerous studies [6, 18, 29, 30]. The use of these nitrogen-alloyed steels at ambient temperatures could provide economic advantages

- their enhanced strength properties enable cross-section reduction in components and structures, ultimately can leading to material savings.

The results of potentiodynamic polarization tests showed that AISI 304L steel, exhibited a higher pitting potential than other steels. The pitting potentials of nitrogen-alloyed steels Cr17Mn9Ni3N and 05Cr18Mn10Ni3N were lower than that of AISI 304L but higher than that of AISI 321 steel. Among the nitrogen-alloyed steels, 05Cr18Mn10Ni3N steel, with its elevated carbon content, demonstrated the lowest pitting potential values.

Several methods exist to enhance the corrosion resistance of austenitic stainless steels through different combinations of alloying elements, with chromium, molybdenum, and nitrogen being the primary ones. The study [6] provides examples of those combinations under "The Cost of Corrosion Resistance." To date, considering current prices of alloying materials for improving steel corrosion resistance, nitrided chromium still remains the most cost-effective option. Table 7 presents the calculated production costs of the steels for vacuum induction melting (VIM) in conditions using pure raw materials (prices data as of mid-2025). In actual industrial practice, prices for these steels are typically 2-2.5 times lower than these calculations, as the production of stainless steels rarely use pure raw materials. However, the proportional relationships between the cost components remain largely consistent.

Table 7. Estimated production cost of the investigated steels based on pure raw material prices (prices data as of mid-2025)

N	Grade	Cost, USD
	Cr17Mn9Ni3N	2855
	05Cr18Mn10Ni3N	2769

3	AISI321	3912
4	AISI304L	3836

The production cost of 05Cr18Mn10Ni3N steel was the lowest due to its minimal nickel content and the partial ability to use medium-carbon ferroalloys. The cost of AISI 321 steel was also slightly higher than AISI 304L, likewise because of its elevated nickel content and the addition of titanium. Overall, for the investigated steels, the calculations confirm that the use of nitrogen as a substitute for nickel remains highly economically advantageous.

5. Conclusions

In the present work, the structure, mechanical properties, and corrosion resistance of low-nickel nitrogen-alloyed austenitic stainless steels (Cr17Mn9Ni3N and 05Cr18Mn10Ni3N) were investigated to assess their viability as cost-effective alternatives to conventional AISI 304L and AISI 321 grades. Based on the experimental results, the following conclusions were drawn:

1. According to thermodynamic calculations, nitrogen-alloyed low-nickel steels exhibit a more stable austenitic structure compared to conventional steels, with a lower probability of high-temperature ferrite formation. However, the likelihood of sigma-phase formation in nitrogen-alloyed steels is higher.

2. Investigated steels achieve a good combination of strength and ductility at room temperature, retaining impact toughness comparable to that of conventional austenitic steels. This enhancement is attributed to solid-solution strengthening provided by interstitial nitrogen. A key limitation is their severely diminished impact toughness at cryogenic temperatures (-196°C), a consequence of the elevated ductile-to-brittle transition temperature induced by high nitrogen content and insufficient nickel levels to maintain austenite toughness.

3. AISI 304L steel, exhibited a higher pitting potential than other steels. The pitting potentials of nitrogen-alloyed steels Cr17Mn9Ni3N and 05Cr18Mn10Ni3N were lower than that of AISI 304L but higher than that of AISI 321 steel.

4. A comprehensive cost-benefit analysis confirms that substituting nickel with nitrogen offers substantial economic advantages. Nitrogen-alloyed steels represent a cost-effective alternative for applications at ambient temperatures, particularly for components requiring high strength and corrosion resistance.

References:

1 P. Yrjölä (Ed.), *Stainless Steel Hollow Sections Handbook*, Finnish Constructional Steelwork Association Ltd., 2008.

2 Outokumpu Oyj, *Handbook of Stainless Steel*, Avesta Research Centre, (n.d.). Retrieved from https://www.outokumpu.com

3 J. Charles, J.-D. Mithieux, J. Krautschick, N. Suutala, J. Simón, B. Hecke, T. Pauly, A new European 200 series standard to substitute 304 austenitics, *Metallurgical Research and Technology*, 106(4) (2009) pp. 123–134. https://doi.org/10.1051/metal/2009019

4 International Stainless Steel Forum (ISSF), "New 200-series" steels: an opportunity or a threat to the image of stainless steel?, Technical Guide No. 5, ISSF, Brussels, 2005.

5 J. Charles, The new 200-series: an alternative answer to Ni surcharge?, Rev. Met. Paris, Vol. 104, N°6 (2007), pp. 308-317. https://doi.org/10.1051/metal/2009019

6 M. O. Speidel, Nitrogen Containing Austenitic Stainless Steels, *Materials Science and Engineering Technology*, 37(10) (2006) pp. 875–880. https://doi.org/10.1002/mawe.200600068

7 O. S. Muradyan, S. O. Muradyan, Melting of High-Nitrogen Austenitic Steels at Atmospheric Pressure, *Metallurgist*, 63(7–8) (2019) pp. 667–671. https://doi.org/10.1007/s11015-019-00904-w

8 J.-H. Shin, J.-Y. Song, Y.-W. Ma, Effects of annealing temperature on microstructural evolution and mechanical properties in cold-rolled high-nitrogen austenitic steel, *Metals*, 14(4) (2024) 389. https://doi.org/10.3390/met14040389

9 H.-B. Li, Z.-H. Jiang, Z.-R. Zhang, Y. Yang, Effect of grain size on mechanical properties of nickel-free high nitrogen austenitic stainless steel, *Journal of Iron and Steel Research, International*, 16(1) (2009) pp. 58–61. https://doi.org/10.1016/S1006-706X(09)60011-X

10 B. Leffler, *Stainless Steels and Their Properties*, Outokumpu, (n.d.). Retrieved from http://www.outokumpu.com

11 Yu. V. Kuznetsov, O. S. Muradyan, S. O. Muradyan, Development of high-strength corrosion resistant austenitic steel for oil equipment shafts, *Metallurgist*, 65(7–8) (2022) pp. 1–5. https://doi.org/10.1007/s11015-022-01251-z

12 Ts. Rashev, A. Eliseev, L. Zhekova, P. Bogev, High-Nitrogen Steel, *Steel in Translation*, 49(7) (2019) pp. 433–439. https://doi.org/10.3103/S0967091219070106

13 V. Kostina, M. Kostina, Welding of high-nitrogen austenitic steels (Review), *Inorganic Materials: Applied Research*, 14(5) (2024) pp. 1152–1164. https://doi.org/10.1134/S2075113323050209

14 K. Yang, Y. Ren, Nickel-free austenitic stainless steels for medical applications, *Science and Technology of Advanced Materials*, 11(1) (2010) 014105 13 pp. https://doi.org/10.1088/1468-6996/11/1/014105

15 T. V. Rashev, *High Nitrogen Steels. Metallurgy under Pressure*, Bulgarian Academy of Sciences, 1995, 253 pages

16 Y. Katada, K. Hirose, M. Kumagai, *Nickel-saving Type High Nitrogen Austenitic Stainless Steel*, Springer, 2022, 99 pp.. https://doi.org/10.1007/978-4-431-56927-5

17 H. Li, Z. Jiang, M. Shen, et al., High nitrogen austenitic stainless steels manufactured by nitrogen gas alloying and adding nitrided ferroalloys, *Journal of Iron and Steel Research, International*, 14(3) (2007) pp. 56–60. https://doi.org/10.1016/S1006-706X(07)60045-4

18 V. G. Gavriljuk, H. Berns, *High Nitrogen Steels: Structure, Properties, Manufacture, Applications*, Springer-Verlag, 1999. 378 pp. https://doi.org/10.1007/978-3-662-03760-7

19 S. Muradian, M. Liu ,Y. Sun, Effect of aging on the structure and mechanical properties of austenite stainless steel N50 alloyed with nitrogen, niobium and vanadium, *Materials Research Express*, 11(7) (2024) 076508 10 pp. https://doi.org/10.1088/2053-1591/ad5cd7

20 A. E. Shelest, V. S. Yusupov, M. M. Perkas, S. O. Muradyan, M. A. Kaplan, Effect of alternating cold elastoplastic deformation on austenitic decomposition during tension of 08Kh18N10 steel, *Russian Metallurgy (Metally)*, 2022(1) (2022) pp. 29–34. https://doi.org/10.1134/S0036029522010104

21 Essoussi, H., Ettaqi, S., Essadiqi, E, On the Prediction of Stacking Fault Energy on Medium MN Steels. Phys. Metals Metallogr. 122, pp. 1507–1512 (2021). https://doi.org/10.1134/S0031918X21140076

22 Essoussi H., Ettaqi S., Essadiqi E.H., From the alloy design to the microstructural and mechanical properties of medium manganese steels of the third generation of advanced high strength steels, Journal of Mining and Metallurgy,

Section B: Metallurgy 2024 Volume 60, Issue 3, pp. 339-352, https://doi.org/10.2298/JMMB240601028E

23 A. Frehn, E. Ratte, and W. Bleck, “Influence of temperature and strain rate on the mechanical properties and the formability of the austenitic stainless steel 1.437 containing manganese and nitrogen,” in Proceedings of 7th International Conference on High Nitrogen Steels (Ostend, 2004), pp. 447–456

24 B. Hwang, T.-H. Lee, S.-J. Kim, Effects of deformation-induced martensite and grain size on ductile-to-brittle transition behavior of austenitic 18Cr10Mn-N stainless steels, *Metals and Materials International*, 16(6) (2010) 905–911. https://doi.org/10.1007/s12540-010-1208-z

25 B. Hwang, T.-H. Lee, S.-J. Kim, Effect of alloying elements on ductile-to-brittle transition behavior of high-interstitial-alloyed 18Cr10Mn austenitic steels, *Procedia Engineering*, 10 (2011) pp. 409–414. https://doi.org/10.1016/j.proeng.2011.04.069

26 R. Mohammadzadeh, A. Akbari, M. Mohammadzadeh, Impact toughness properties of nickel- and manganese-free high nitrogen austenitic stainless steels, *Metallurgical and Materials Transactions A*, 47(8) (2016) pp. 4029–4042. https://doi.org/10.1007/s11661-016-3742-x

27 Y. Tomota, Y. Xia, K. Inoue, Mechanism of low temperature brittle fracture in high nitrogen bearing austenitic steels, Acta Materialia, 46(5) (1998) pp. 1577–1587. https://doi.org/10.1016/S1359-6454(97)00350-9

28 A. A. Tiamiyu, U. Eduok, J. A. Szpunar, A. G. Odeshi, Corrosion behavior of metastable AISI 321 austenitic stainless steel: investigating the effect of grain size and prior plastic deformation on its degradation pattern in saline media, *Scientific Reports*, 9 (2019) 12116 18 pp. https://doi.org/10.1038/s41598-019-48594-3

29 D. Manova, D. Hirsch, E. Richter, S. Mändl, H. Neumann, B. Rauschenbach, Microstructure of nitrogen implanted stainless steel after wear experiment, *Surface and Coatings Technology*, 201(19–20) (2007) pp. 8329–8333. https://doi.org/10.1016/j.surfcoat.2006.10.060

30 L. Valentini, A. D. Schino, J. M. Kenny, S. D. Rosa, L. Lozzi, S. Santucci, et al., Wear resistance of fine-grained high nitrogen austenitic stainless steel coated with amorphous carbon films: the soft X-ray spectroscopy approach, *Tribology Letters*, 16(1–2) (2004) pp. 51–58. https://doi.org/10.1023/B:TRIL.0000009714.09197.25

Declaration of Competing Interest

The authors declare that they have no known competing financial interests or personal relationships that could have appeared to influence the work reported in this paper.

Acknowledgements

This work was supported by the Zhejiang Provincial Department of Science and Technology, China [Project No. 2025C01153].